Development of a rocket target RT-400m for medium-range air defence system

Hari prasanna Manimaran[1]*, Algimantas Fedaravičius[2]

[1]Department of Transport Engineering, Kaunas University of Technology, Lithuania

[2]Department of Transport Engineering, Kaunas University of Technology, Lithuania

*Corresponding author

Abstract.

Live fire exercise is carried out to improve the ability of the personnel to operate military hardware. Rocket targets are used in this exercise to mimic high-speed targets. The objective of the research is to develop a realistic and adaptable target capable of simulating oncoming enemy aircraft, rockets, and missiles allowing trainees to engage in accurate and immersive training situations. RT-400M is a target rocket developed as a medium-range rocket target. The RT-400M is designed to reach a maximum range of 20 km and an altitude of 10 km. It is an upgraded version of the RT-400. A numerical ballistic study of many feasible models of a rocket motor is performed to obtain the requirement. Two and four-motor rockets are studied, and the four-motor type is chosen for the final model. The aerodynamic analysis is conducted to modify the shape and ensure its stability throughout the trajectory. Drag and moments are calculated for the subsonic and supersonic speed regimes. The experimental model for the live firing exercise is produced based on the research data. The design and development process are presented in this study.

Keywords: Aerodynamic analysis, Ballistics, Drag force, Rocket target, RT-400M.

1. Introduction

With the rapid advancement of defence technology, adequate training is required for operating defence hardware. Live fire exercises are frequently used to test military equipment, such as air defence systems. Personnel requires targets that represent genuine incoming enemy military hardware during these drills to recreate realistic scenarios and prepare them for battle conditions. Precise practice helps individuals become proficient operators, and targets that mimic hostile aircraft or rockets are used for this reason (Bakirci, 2021).

Initially, virtual and slow-moving targets are used for practice, but other sorts of targets are also employed depending on the situation. The primary purpose of targets is to serve as a practice bullseye, and most of them are meant to be destroyed during practice. Targets can be used for land, sea, and air defence, and most militaries create their targets for their practices (Fedaravičius et al., 2015).

There are three types of targets: fixed-wing aircraft, UAVs, and rocket targets. Some targets are turbojet-powered drones and missile targets constructed from missile parts that lack warheads. Other targets are designed in response to special needs. However, drone targets are incapable of simulating the situation for fast-moving missiles and fighter aircraft, and thus rocket targets are utilised instead. These targets are propelled by a rocket motor, which is typically powered by solid propellant.

Trainees must be trained to acquire, lock, and destroy the target. Therefore, rocket targets are typically slower than the actual missile or aerial vehicle. Identifying fast-moving objects is challenging in the early stages of training. As a result, the target's speed is chosen to match the trainee's response time. In contrast to drones, which may be reused, rocket targets are used once and mainly destroyed during drills. The rocket is stored as a secondary target in drones and is expelled to mimic the missile. As rocket-assisted take-off (RATO), certain drones employ rockets for the initial stage. Drone targets are difficult to maintain and cannot be used in all-weather situations, but solid-propellant rocket targets may be fuelled and kept for a longer amount of time with less maintenance.

Given all the advantages of employing rocket targets for military exercises, the rocket must be designed and tested. Internal and exterior ballistics are considered while building rocket targets. Internal ballistics is concerned with the properties of the propulsion system, whereas external ballistics is concerned with the flight of the projectile. External ballistics gives fundamental characteristics such as thrust, velocity, acceleration, altitude, flight angles, and range to optimise the target for individual requirements. The design may be modified to meet the requirements.

This study focuses on analyzing a rocket target for use in air defence systems, especially the RT-400M, which was designed and produced by the Kaunas University of Technology, Institute of Defense Technology. The RT-400M has a range that was extended from the previous variant by optimizing the propulsion system. A performance study is required when making changes to any system, and in this situation, external ballistics influence the performance of the rocket target.

Based on data from the single motor of the RM-12K, multiple motor grids can be studied to meet different range requirements. To increase the range from short to medium, additional motors are added. For this research, a mid-range rocket target with four motors will be used to achieve a range of 15-20 km. In this research, the process of developing the rocket target is discussed. From computational methods used for designing the rocket, and computational results are discussed.

2. Methodology

The development of rocket targets consists of computational design and analysis and prototype testing. Computational design is cost-effective and provides a more precise result in a shorter time. The steps involved in computational design are discussed.

2.1 Computational design

The RT-400M is a 5.4-meter-long rocket with a 0.41-meter diameter of body. The 100mm increment from the previous version to accommodate the four-motor propulsion block. The aerodynamic analysis is carried out to compare the different nose profiles. The rocket's maximum velocity needs to be restricted to a low supersonic regime. So, the parabolic nose shape is adapted to boost subsonic flow performance.

The aft section has four trapezoidal fins grouped in a clipped delta configuration. This profile gives stability for all speed regimes of the rocket by maintaining a location of the centre of pressure behind the centre of mass. Four solid propellant rocket motors are positioned in a parallel arrangement at the rear end for propulsion. Due to the addition of a propulsion block, pull the CG behind the aerodynamic centre. Additional weights are added to the nose cone and front end of the rocket to compensate for the stability. 0.5 calibre stability is maintained for the first stage of the rocket and 1.2 calibre stability is obtained for the second stage due to first-stage fuel burn and reduction in fuel mass.

The entire diameter including the fins is 1.2 metres, and the cross-sectional area of the rocket body is 0.132 square metres. A CAD model has been improved with geometry cleaning and made watertight for fluid flow analysis. The computational model of RT-400M is shown in Figures 1 and 2.

The propulsion unit with four motors is arranged in a parallel configuration and is modelled using CAD software. Based on the computational design, a working model is manufactured as shown in Figure 3. Analysis of various nose cones (Bakirci, 2021) and fin geometries are analysed for optimum aerodynamic performance and stability(Cook, 2013b).

Table 1: specification of RT-400M

s.no	Property	values
1	Length of the rocket (m)	5.4
2	Diameter of the target (m)	0.41
3	Rocket mass (kg)	104
4	Maximum flight range (km)	20
5	Maximum flight altitude (km)	10
6	Velocity range of the rocket (m/s)	280-350

Figure 1: side and front view of RT-400M
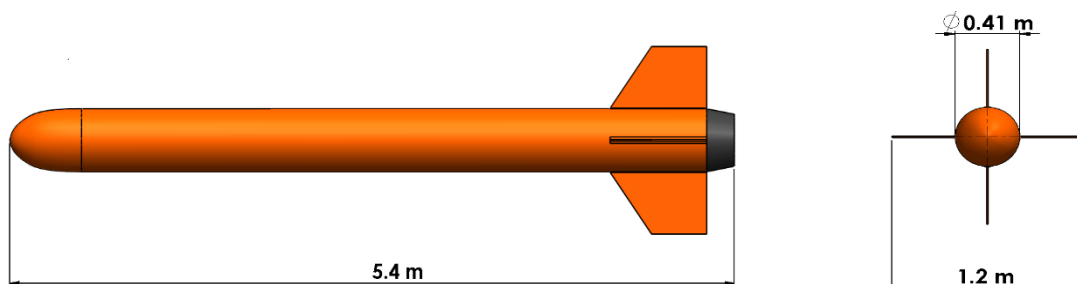
Figure 2: Computational model of RT-400m with four motor arrangements.
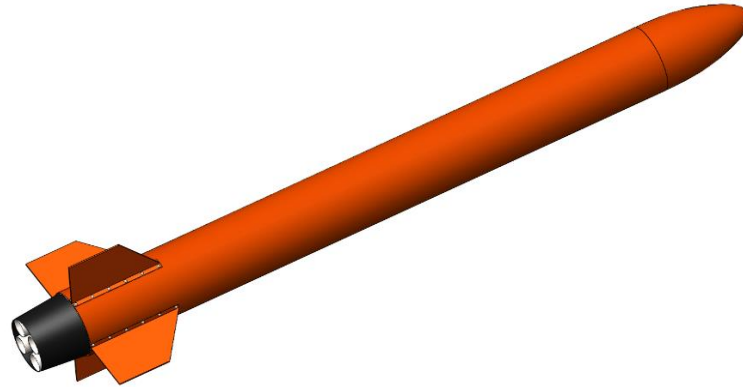

Figure 3: Four RM-12K motors arranged in a parallel configuration propulsion unit.

2.2 Numerical analysis

To analyze the fluid flow over an RT-400M, the numerical technique of computational fluid dynamics is applied. This method is less expensive and produces more exact results. CFD techniques compared to experimental analysis can reduce the total design cycle time and cost(Wilcox & Wilcox, 2006).

For fluid analysis, the Ansys Fluent numerical tool is utilized. The computational model is imported into the design modeller and an 8-meter-diameter fluid domain is generated with an 8-meter-long upstream and 25-meter-long downstream fluid domain built around the body.

A longer downstream is constructed to examine the wake and pressure shift caused by the body. The fluid domain is meshed using a combination of tetrahedral and hexahedral meshes (Ito & Nakahashi, 2004). A structured mesh type with 10 inflating layers is designed around the rocket body to detailly evaluate the boundary layer. A higher concentration of mesh is built towards the body's edge to compute and visualize the forces. There are a total of 510,004 elements produced.

The meshed domain is imported into the workspace to create an analytical configuration based on a constant pressure solution. The solver's viscous model with the k-omega equation is chosen because it accurately predicts pressure gradients and boundary layer separation, with SST equations for correcting overprediction. The fluid domain is air with mean sea-level conditions for subsonic flow, whereas the ideal gas condition for density and the Sutherland two-coefficient model for viscosity is employed for supersonic flow (Cook, 2013).

For the boundary condition, several velocity magnitudes from subsonic to supersonic Mach values are considered, with 5% turbulence intensity (Sivasubramanian et al., 2006). For an inlet, the fluid condition of the velocity inlet is applied to the front face of the fluid domain. The back end is chosen as a zero-pressure outlet. The rocket body and far-field boundary are chosen as the walls with the no-slip condition (Kundu et al., 2016). Reference values are taken from the intake for calculation. The mean sea level is used to compute density, pressure, temperature, and viscosity. A Y-plus of 300 is applied (Miltner et al., 2015).

In pressure-velocity coupling approaches, a coupled scheme with a Rhie-Chow distance-based flux type is used. Cell-based least squares discretization with the second-order upwind type is applied. The finite-volume technique is employed for numerical analysis, while the Reynolds-averaged Navier-Stokes equation in conservation form is used for simulation (Tu et al., 2018).

Reynolds averaged Navier-strokes equation in conservation form is used for running simulation. Mass and momentum equation is shown in equations 1 and 2,

$$\frac{\partial \rho}{\partial t} + \nabla(\rho u) = 0 \tag{1}$$

$$\frac{D(u_i)}{Dt} = \frac{\partial u_i}{\partial t} + U_j \frac{\partial u_i}{\partial x_j} = -\frac{1}{\rho}\frac{\partial P}{\partial x_i} + \upsilon \frac{\partial^2 u_i}{\partial x_j^2} + F_i \tag{2}$$

Where ρ is the density of the fluid; u is the fluid velocity, t is time, P is the mean static pressure, F_i is the external force vector, v is the local kinematic, u_i is the velocity vector, and x_j is the position vector.

x component

$$\rho \frac{D\bar{u}}{Dt} = \rho \left[\frac{\partial}{\partial x}\left(\overline{u^2}\right) + \frac{\partial}{\partial y}\left(\overline{uv}\right) + \frac{\partial}{\partial z}\left(\overline{uw}\right) \right]$$

$$= \rho g_x - \frac{\partial \bar{P}}{\partial x} + \frac{\partial}{\partial x}\left[\mu \frac{\partial \bar{u}}{\partial x} - \rho \overline{u'^2} \right] + \frac{\partial}{\partial y}\left[\mu \frac{\partial \bar{u}}{\partial y} - \rho \overline{u'v'} \right] + \frac{\partial}{\partial z}\left[\mu \frac{\partial \bar{u}}{\partial z} - \rho \overline{v'w'} \right]$$

(3)

y component

$$\rho \frac{D\bar{v}}{Dt} = \rho \left[\frac{\partial}{\partial x}\left(\overline{uv}\right) + \frac{\partial}{\partial y}\left(\overline{v^2}\right) + \frac{\partial}{\partial z}\left(\overline{vw}\right) \right]$$

$$= \rho g_y - \frac{\partial \bar{P}}{\partial y} + \frac{\partial}{\partial x}\left[\mu \frac{\partial \bar{v}}{\partial x} - \rho \overline{u'v'} \right] + \frac{\partial}{\partial y}\left[\mu \frac{\partial \bar{v}}{\partial y} - \rho \overline{v'^2} \right] + \frac{\partial}{\partial z}\left[\mu \frac{\partial \bar{v}}{\partial z} - \rho \overline{v'w'} \right]$$

(4)

z component

$$\rho \frac{D\bar{w}}{Dt} = \rho \left[\frac{\partial}{\partial x}\left(\overline{uw}\right) + \frac{\partial}{\partial y}\left(\overline{vw}\right) + \frac{\partial}{\partial z}\left(\overline{w^2}\right) \right]$$

$$= \rho g_z - \frac{\partial \bar{P}}{\partial z} + \frac{\partial}{\partial x}\left[\mu \frac{\partial \bar{w}}{\partial x} - \rho \overline{u'w'} \right] + \frac{\partial}{\partial y}\left[\mu \frac{\partial \bar{w}}{\partial y} - \rho \overline{v'w'} \right] + \frac{\partial}{\partial z}\left[\mu \frac{\partial \bar{w}}{\partial z} - \rho \overline{w'^2} \right]$$

(5)

Where μ is the molecular viscosity, g is the acceleration due to gravity.

Turbulence kinetic energy (k)

$$\frac{\partial}{\partial t}(\rho k) + \frac{\partial}{\partial x_j}(\rho u_j k) = \rho P - \beta^* \rho \omega k + \frac{\partial}{\partial x_j}\left[\left(\mu + \sigma^* \frac{\rho k}{\omega} \right) \frac{\partial k}{\partial x_j} \right]$$

(6)

$$P = \tau_{ij} \frac{\partial u_i}{\partial x_j}$$

(7)

Where k is turbulence kinetic energy, σ, β* is closure coefficients, and τ is the specific Reynolds stress tensor.*

9

The specific rate of dissipation (ω)

$$\frac{\partial}{\partial t}(\rho\omega) + \frac{\partial}{\partial x_j}(\rho u_j \omega) = \alpha \frac{\omega}{k} P - \beta \rho \omega^2 + \sigma_d \frac{\rho}{\omega} \frac{\partial k}{\partial x_j} \frac{\partial \omega}{\partial x_j} + \frac{\partial}{\partial x_j}\left[\left(\mu + \sigma \frac{\rho k}{\omega}\right)\frac{\partial \omega}{\partial x_j}\right] \tag{8}$$

Where w is the specific dissipation rate, α, β, σ, σ$_d$ closure coefficients.

2.3 Ballistics analysis

A mathematical model was created to determine the external ballistics of a rocket target. The model considers both the active (when the rocket motor is active) and passive (when the rocket motor is burnt off) phases of the trajectory. Due to the low altitude and flight distance of the target rocket, the model makes various simplifying assumptions. As the flight distance and duration are short, the Earth's curvature, Coriolis acceleration, and atmospheric fluctuations were not considered. The rocket target's sideslip angle is small; only the longitudinal plane is examined, and the angle of attack is zero. The flight occurs in a certain layer of the atmosphere, and the air drag in the specified range of velocity must be considered while determining the flight trajectory's characteristics (Janzon & Woodley, 2016).

The internal ballistic analysis is performed numerically and experimentally. The RM-12k rocket motor with 12 kN thrust is experimentally tested and the thrust values are obtained. The chamber pressure is calculated. Internal ballistic simulation with the computational model is performed to obtain thrust values and validated with the experimental results. The ballistic equation used for the analysis is given in the equation 9 to 14.

$$\text{Horizontal distance } x = x_0 + v_0 t \cos\theta - \frac{1}{2}\left(\frac{CD*A*\rho*v_0^2*t^2}{m*g*cos^2\theta}\right) \tag{9}$$

$$\text{Vertical distance } y = y_0 + v_0 t \sin\theta - \frac{1}{2}gt^2 - \frac{1}{2}\left(\frac{CD*A*\rho*v_0^2*t^2}{m*g*cos^2\theta}\right) \tag{10}$$

$$\text{Horizontal velocity } v_x = v_0 \cos\theta - \left(\frac{CD*A*\rho*v_0*t*cos\theta}{m*g}\right) \tag{11}$$

$$\text{Vertical velocity } v_y = v_0 \sin\theta - gt - \left(\frac{CD*A*\rho*v_0*t*sin\theta}{m*g}\right) \tag{12}$$

$$\text{Maximum velocity } v_{max} = v_0 e^{\left(\frac{-gt}{v_0 cos\theta}\right)} - \left(\frac{CD*A*\rho}{2*m*g*cos^2\theta}*t\right) \tag{13}$$

$$\text{Acceleration } a_x = -\frac{CD*A*\rho*v_0*cos^2\theta}{m*g}, a_y = -g - \frac{CD*A*\rho*v_0*sin^2\theta}{m*g} \tag{14}$$

MATLAB Simulink is used to determine the flight trajectory parameters and the rocket target properties. The active and passive phases were assessed, as well as the dependence of the air drag force on velocity and internal ballistic data. The algorithm also accounted for a drop in rocket mass due to fuel consumption during the active phase. The active phase acceleration was around 280 m/s for all launch angles, while the passive phase acceleration varied between 20 and 30 m/s. The velocity of the rocket target varies with the launch angle. Based on the requirement, the rocket must reach 20 km in distance and 10 km in altitude. For different launch angles, the rocket reaches different trajectories and reaches different distances, as shown in Figure 4.

Figure 4: Ballistic result of the four motor RT-400m for various launch angles.
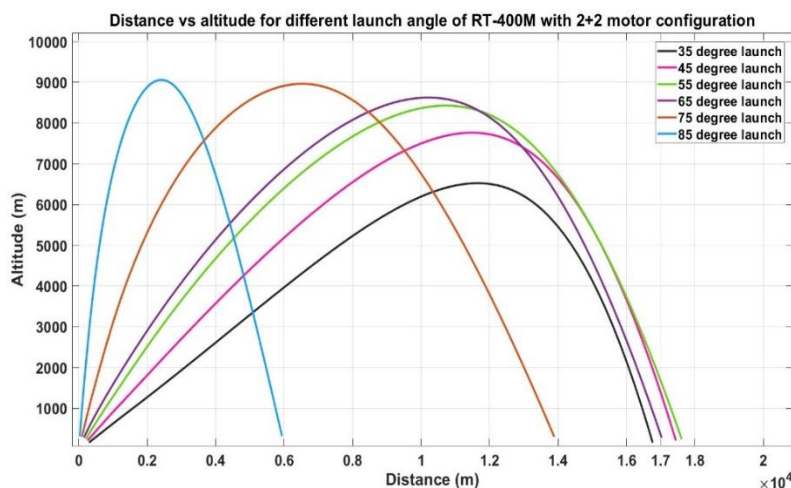
2.4 Design Algorithm

The development of rocket targets designed for medium-range air defence systems follows an iterative process in which computational tools are used for design and analysis to shorten the design iteration cycle and reduce related expenses. By specific operating requirements, a numerical model is developed and rigorously tested using modern computational techniques. To confirm the aerodynamic performance predictions produced from computer simulations, experimental validation is pursued through wind tunnel testing across several speed regimes, assuring the integrity of the modelled aerodynamic behaviour. The iterative refining method includes design improvements targeted at improving the performance characteristics of the rocket targets.
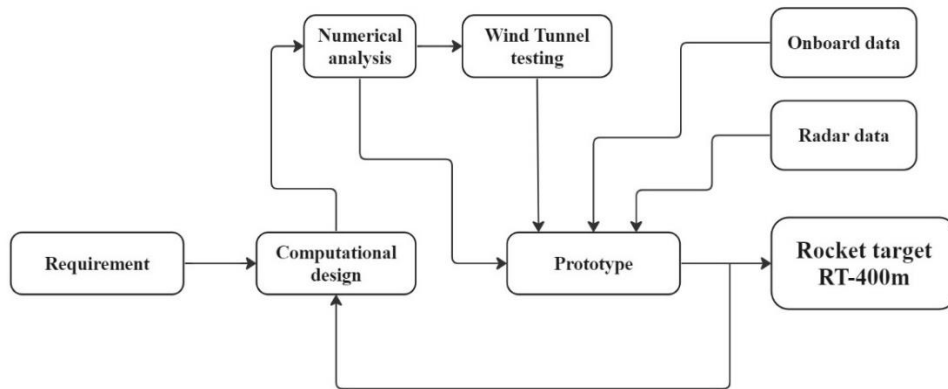
Figure 5: Schematic representation of the design and development of RT-400m.

To this purpose, insights gained from data collected during previous live fire drills are carefully incorporated into design refinement efforts. Figure 5 depicts an iterative feedback loop that allows empirical insights to be assimilated into following design iterations, enabling continual development and refinement in the quest for optimal performance metrics. This integrative approach emphasises the synergistic coupling of computational modelling, experimental validation, and empirical insights gleaned from real-world operational scenarios, resulting in a comprehensive and robust framework for iterative development and optimisation of rocket targets designed for medium-range air defence systems.

2.5 Prototype for the live fire exercise

Figure 6 of this research study illustrates the prototype of the RT-400M model, which has been optimised for live fire exercises. A specialised mobile launch platform has been precisely designed to accommodate and facilitate launches from a variety of angles. This unique platform allows the rocket to be launched from a variety of angles, allowing for the attainment of required distances and heights during training. This transportable launch platform stands out for its ability to be towed by regular road vehicles, which increases its operational versatility and ease of deployment. This strategic design consideration provides accessibility over a wide range of terrains and environments, increasing the usability and accessibility of the RT-400M model for real exercise scenarios. The platform's modular design enables smooth changes to meet various launch parameters based on individual training objectives and operating requirements. As a result, the RT-400M model, together with its specialised transportable launch platform, is a complete and versatile solution designed to meet the demands of live training exercises.
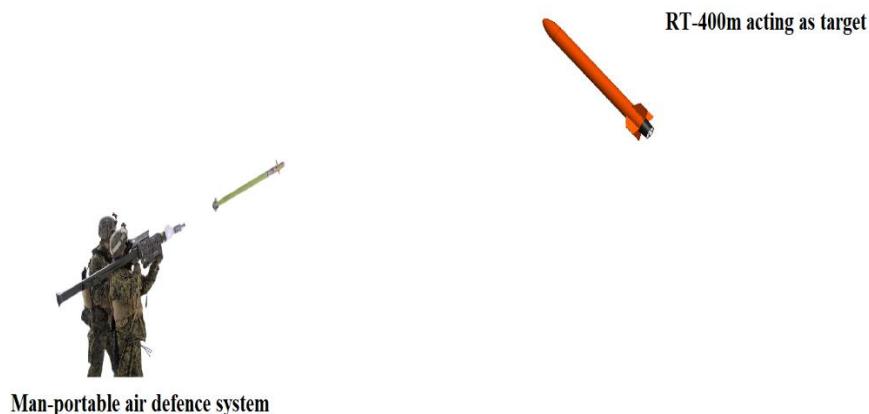
Figure 6: RT-400m prototype for live fire exercise.

2.6 Schematics of the working

The live fire drills provide critical training chances for military troops to practice combat scenarios in realistic settings.

Figure 7: Mission design of RT-400M in live fire exercise.

RT-400m acting as target

Man-portable air defence system

During these exercises, target rockets are used to simulate the trajectory and velocity of genuine enemy projectiles, like as missiles or planes, presenting trainees with realistic combat scenarios.

The drills usually include the deployment and firing of these target rockets, followed by trainees visually recognising and tracking them using air defence guiding systems. Subsequently, trainees engage the target rockets with missiles to intercept and neutralise them. To promote successful training, target rockets are constructed with special properties. Notably, they are designed in bright colours to provide good visibility in a variety of weather circumstances, improving trainees' ability to visually acquire and track them.

3. Conclusion

This study has thoroughly examined the requirement of rocket targets for medium-range air defence systems, looking at several target arrangements. Considerable progress has been made by adding more motors to propulsion systems to optimise rocket targets for short- to medium-range defence systems. The accurate calibration of design parameters to satisfy operational demands has been made possible by utilising computational modelling approaches. Furthermore, thorough ballistic and aerodynamic evaluations have significantly improved the rocket targets' performance capabilities. Alignment with operational needs has been ensured through continuous refinement made possible by the iterative design approach. The creation and production of a prototype for live fire testing, complete with a customised transportable launch platform, is the pinnacle of this study. All of these efforts constitute a major advancement in improving the effectiveness and dependability of rocket targets in medium-range air defence systems.

References

Bakirci, M. (2021). Design and Aerodynamic Analysis of a Rocket Nose Cone with Specific Fineness Ratio. *2021 IEEE 6th International Conference on Actual Problems of Unmanned Aerial Vehicles Development, APUAVD 2021 - Proceedings*, 80–85. https://doi.org/10.1109/APUAVD53804.2021.9615407

Cook, M. V. (2013a). Aerodynamic Modelling. *Flight Dynamics Principles*, 353–369. https://doi.org/10.1016/B978-0-08-098242-7.00012-2

Cook, M. V. (2013b). Aerodynamic Stability and Control Derivatives. *Flight Dynamics Principles*, 371–439. https://doi.org/10.1016/B978-0-08-098242-7.00013-4

Fedaravičius, A., Kilikevičius, S., & Survila, A. (2015). Investigation on the aerodynamic characteristics of a rocket target for the system "Stinger." *Journal of Vibroengineering*, *17*(8), 4490–4495. https://www.extrica.com/article/16142

Ito, Y., & Nakahashi, K. (2004). Improvements in the reliability and quality of unstructured hybrid mesh generation. *International Journal for Numerical Methods in Fluids*, *45*(1), 79–108. https://doi.org/10.1002/FLD.669

Janzon, B. S. G., & Woodley, C. (2016). 29th International Symposium on Ballistics, Edinburgh, Scotland, UK, 9–13 May 2016. *Defence Technology*, *12*(2), A1. https://doi.org/10.1016/J.DT.2016.02.001

Kundu, P. K., Cohen, I. M., & Dowling, D. R. (2016). Boundary Layers and Related Topics. *Fluid Mechanics*, 469–532. https://doi.org/10.1016/B978-0-12-405935-1.00010-1

Miltner, M., Jordan, C., & Harasek, M. (2015). CFD simulation of straight and slightly swirling turbulent free jets using different RANS-turbulence models. *Applied Thermal Engineering*, *89*, 1117–1126. https://doi.org/10.1016/J.APPLTHERMALENG.2015.05.048

Sivasubramanian, J., Sandberg, R. D., Von Terzi, D. A., & Fasel, H. F. (2006). Numerical investigation of flow control mechanisms for drag reduction in supersonic base-flows. *Collection of Technical Papers - 44th AIAA Aerospace Sciences Meeting*, *15*, 10775–10784. https://doi.org/10.2514/6.2006-902

Tu, J., Yeoh, G.-H., & Liu, C. (2018). Governing Equations for CFD: Fundamentals. *Computational Fluid Dynamics*, 65–124. https://doi.org/10.1016/B978-0-08-101127-0.00003-9

Wilcox & Wilcox, David C. (2006). Turbulence Modeling... - Google Scholar. (n.d.). Retrieved February 12, 2024